process (~8 orders of magnitude) or to a classical conformational change. The pathway which leads to the conversion of I_0 to the catenate is very narrow. Fitting together the dpp subunits while unraveling the pentaoxyethylene links from one another and bringing them to the back of the phenanthroline nuclei must be a slow process as long as a solvated metal is present. The compactness of the many intermediate microstates encountered in the course of the transformation of I_0 to M(cat-30) probably requires simultaneous release of two or more solvent molecules, which drastically slows down the overall complexation reaction.

Until now, all the physical methods used in order to investigate the new class of ligands formed by catenands have shown that those molecules behave as *single chemical species*. The present study illustrates this characteristic property. Kinetically, cat-30 behaves as a *single ligand* and not as two dap subunits. As suggested by the reaction schemes of Figure 5, the dpp fragments do not ignore each other. If cat-30 would act as an ensemble of two separate coordinating molecules, it would probably lead to dinuclear species (each dpp fragment bound to a metal center) at some stage during the complexation reaction. This hypothesis has been checked experimentally by using a large excess of ligand with respect to Li^+, whereas the experimental data discussed above have been obtained in a completely inverse situation ([ligand]/[metal cation] < 0.1). Two steps are still clearly observed although the formation of dimetallic complexes is strongly disfavored.[29]

In summary, the present kinetic study points to the unusual properties of catenands with respect to the reaction pathway leading to catenates. In particular, the catenane nature of the ligand cat-30 leads to a surprising two-step reaction for Li^+, Zn^{2+}, Cd^{2+}, and Co^{2+} complexation. The second step observed is assigned to the gliding motion of one ring within the other, such a process being responsible for the complete rearrangement of the organic skeleton. Owing to the corresponding narrow reaction pathway and to the rigidity and compactness of the final state, this reorganization is remarkably slow.

Acknowledgment. We thank the CNRS for its constant financial support.

Registry No. m-30, 90030-13-0; dap, 89333-97-1; Cu^+, 17493-86-6; Ag^+, 14701-21-4; Li^+, 17341-24-1; Cd^{2+}, 22537-48-0; Zn^{2+}, 23713-49-7; Co^{2+}, 22541-53-3; $Cu(dap)^+$, 112195-98-9.

(29) Although the "dimetallic hypothesis" represented on the following scheme seems to be highly improbable, it is difficult to totally exclude it at the present stage. We thank Prof. D. W. Margerum for stimulating discussions regarding this problem.

Scheme I

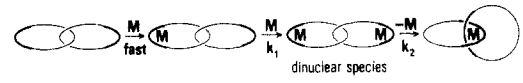

Ruthenium(IV)–Oxo Complexes: The Novel Utilization of Tertiary Pnictogen Ligands

Mary E. Marmion and Kenneth J. Takeuchi*

Contribution from the Department of Chemistry, SUNY at Buffalo, Buffalo, New York 14214.
Received July 22, 1987

Abstract: The novel complexes $[(bpy)_2(PnR_3)Ru^{IV}(O)](ClO_4)_2$ (where bpy = 2,2′-bipyridine and PnR_3 = tertiary phosphine or arsine) have been generated from the analogous ruthenium(II)–aquo species, through electrochemical means or by the addition of two equivalents of cerium(IV). Characterization of the ruthenium(II)–aquo and ruthenium(IV)–oxo complexes was accomplished through UV–vis spectroscopy, IR spectroscopy, ^{18}O labeling experiments, NMR spectroscopy, cyclic voltammetry, coulometry, and conductivity measurements. These complexes are stable both in the solid state and in various solutions, where the phosphine and arsine ligands do *not* undergo oxidation by the ruthenium(IV)–oxo center. Cyclic voltammetric measurements of the ruthenium(II)–aquo complexes are consistent with the following redox couples: $Ru^{IV}{=}O/Ru^{III}{-}OH/Ru^{II}{-}OH_2$, which can be described as two sets of concomitant one-electron, one-proton transfers. The ruthenium(IV)–oxo complexes act as selective oxidation reagents toward organic substrates, where the nature of the pnictogen ligand greatly affects the rate of substrate oxidation. In addition, the use of a pnictogen ligand cis to the oxo moiety in these complexes simplifies the mechanism of substrate oxidation relative to other ruthenium-based oxidants. Finally, pnictogen ligands exert unusual effects on the redox chemistry of ruthenium(IV)–oxo complexes, including hydrophobic selectivity and aerobically driven substrate oxidation catalysis.

Ruthenium–oxo/aquo complexes have proven to be very suitable in the design of redox catalysts for a variety of reasons. First, transition metals are useful catalysts in redox reactions since one or more oxidation states are frequently available as a source of or sink for electrons, thus enabling multiple electron transfers to occur. In addition, the substitutionally inert nature of ruthenium[1-3] allows for chemically reversible electron transfer uncomplicated by ligand exchange. Therefore, ruthenium complexes tend to retain their integrity in solution and are relatively easy to study. Finally, the oxo–aquo ligands provide for rapid proton transfer concomitant with electron transfer permitting the accessibility of several oxidation states via gain or loss of protons.[4,5]

Previously, we reported the first successful syntheses and characterizations of ruthenium(IV)–oxo complexes that contain tertiary phosphine ligands in a position cis to the oxo ligand.[6]

(1) Margerum, D. W.; Cayley, G. R.; Weaterburn, D. C.; Pagenkopf, G. K. *Coordination Chemistry*; American Chemical Society: Washington, DC, 1978; ACS Monography 174, Vol. 2, Chapter 1.
(2) Seddon, E. A.; Seddon, K. R. *The Chemistry of Ruthenium*; Elsevier: New York, 1984.
(3) Griffith, W. P. *The Chemistry of Rarer Platinum Metals*; Interscience: London, 1967.
(4) (a) Takeuchi, K. J.; Samuels, G. J.; Gersten, S. W.; Gilbert, J. A.; Meyer, T. J. *Inorg. Chem.* **1983**, *22*, 1407–1409. (b) Takeuchi, K. J.; Thompson, M. S.; Pipes, D. W.; Meyer, T. J. *Inorg. Chem.* **1984**, *23*, 1845–1851.
(5) (a) Moyer, B. A.; Meyer, T. J. *J. Am. Chem. Soc.* **1978**, *100*, 3601–3603. (b) Moyer, B. A.; Meyer, T. J. *Inorg. Chem.* **1981**, *22*, 436–444.
(6) Marmion, M. E.; Takeuchi, K. J. *J. Am. Chem. Soc.* **1986**, *108*, 510–511.

0002-7863/88/1510-1472$01.50/0

Phosphine ligands were chosen to modify the oxidation chemistry of ruthenium–oxo complexes because these ligands provide a broad variety of well-characterized steric and electronic ligand properties.[7-11] Although tertiary phosphine ligands are extremely susceptible to oxidation, these ligands prove to be very stable when located in the coordination sphere of the high oxidation state ruthenium center. In this manner, the diverse chemistry of phosphine ligands, which have conventionally been used in the syntheses of low valent organometallic complexes, is exploited in the design of fundamentally new, very potent oxidation agents that possess a wide variety of metal redox potentials, as well as steric and hydrophobic ligand variability. For example, we have determined that these complexes act as oxidation reagents toward organic and inorganic substrates, where the nature of the phosphine ligand greatly affects both the product distribution and rate of substrate oxidation.[13a] In addition, we have reported the unusual hydrophobic selectivity of primary alcohol oxidation by phosphine–ruthenium(IV)–oxo complexes, where a linear relationship between the hydrophobicity of the alcohol and the rate of oxidation is observed.[13b] Finally, we have reported the aerobically driven catalytic oxidation of olefins by phosphine–ruthenium(II)–aquo complexes, where the steric properties of the tertiary phosphine ligand play a key role in the catalytic activity of the ruthenium(II) center.[13c]

These ruthenium(IV)–oxo complexes, $[(bpy)_2(PnR_3)Ru^{IV}(O)](ClO_4)_2$ (where bpy = 2,2′-bipyridine and PnR_3 = PMe_3, PEt_3, $P(i\text{-}Pr)_3$, PCy_3, PPh_3, $AsPh_3$),[12] are remarkably stable both in the solid state and in solution, where the phosphine ligands do not undergo oxidation by the ruthenium(IV)–oxo center. Thus, these complexes provide a unique opportunity to fully characterize and control the redox chemistry of ruthenium(IV)–oxo complexes. In this paper, we describe in detail the preparation and characterization of pnictogen–ruthenium(IV)–oxo and pnictogen–ruthenium(II)–aquo complexes.

Experimental Section

Materials. House distilled water was employed throughout and was passed through Barnstead HN Combination (D8922) and HN Organic Removal (D8904) purification cartridges before use. HPLC–GC/MS methylene chloride (Fisher Scientific) and HPLC acetonitrile (Fisher Scientific) were used without further purification for both electrochemical and spectral measurements. $RuCl_3 \cdot 3H_2O$ and $AgClO_4$ were obtained from Johnson Matthey Inc., and 2,2″-bipyridine was obtained from Aldrich Chemical Co. Phosphine ligands were purchased from Aldrich or Strem Chemical and were used as received. Ceric perchlorate solution, 0.5 N in 6 N perchloric acid, was obtained from G. F. Smith Chemical Co. All other simple salts, solvents, acids, and bases were of reagent quality and were used without further purification.

Measurements. UV–vis spectra were obtained in quartz cells on a Bausch and Lomb Spectronic 2000 spectrophotometer. Beer's law was verified by using three different sample concentrations, and the reported extinction coefficient values are generally an average of two measurements that agreed within 10%. IR spectra were obtained as Nujol mulls on KBr plates with a Perkin-Elmer 457 Grating spectrophotometer. ^1H and ^{13}C NMR spectra were measured with a JEOL FX90Q Fourier transform spectrometer, with either deuteriated chloroform or methylene chloride as the solvent. Conductivity data were measured by employing a YSI Model 31 conductivity bridge. Elemental analyses were performed by Atlantic Microlab.

Electrochemical measurements were conducted with an IBM EC/225 voltammetric analyzer, and current–voltage curves were recorded with a Houston Instruments Model 164 recorder. Cyclic voltammetric work was performed in one-compartment cells with a platinum, glassy carbon, or carbon paste working electrode (BAS Bioanalytical Systems), a platinum wire auxiliary electrode, and a saturated sodium chloride calomel reference electrode (SSCE). For cyclic voltammetric experiments run in methylene chloride and acetonitrile, the supporting electrolyte was tetra-*n*-butylammonium tetrafluoroborate (Bu_4NBF_4), which was prepared and purified by standard methods[14] and was used in 0.1 M concentrations for all solutions. The pH values of aqueous solutions employed in electrochemical experiments were buffered at an ionic strength of 0.1 M by HNO_3 and $NaNO_3$ (pH 0–2), potassium hydrogen phthalate and HNO_3 (pH 2–4), potassium hydrogen phthalate and NaOH (pH 4–6), KH_2PO_4 and NaOH (pH 6–8), borax and HNO_3 (pH 9–11), Na_2HPO_4 (pH 11–12), and NaOH (pH 13–14). The $E_{1/2}$ values for reversible couples were calculated from half the difference between E_p values for the cathodic and anodic waves from cyclic voltammetry. Reticulated vitreous carbon or Pt-gauze electrodes were utilized as the working electrodes in exhaustive electrolysis experiments which were performed in two-compartment fritted cells.

***cis*-$Ru^{II}(bpy)_2Cl_2 \cdot 2H_2O$.** The following modification of a literature preparation[15] was employed to give pure product in good yields. $RuCl_3 \cdot 3H_2O$ (1.56 g, 5.97 mmol) was dissolved in reagent grade dimethylformamide (10 mL). Lithium chloride (1.48 g, 34.9 mmol) and 2,2′-bipyridine (1.87 g, 12 mmol) were then added, and the resulting mixture was deaerated with nitrogen for 5 min. The solution was refluxed for 6 h and was stirred magnetically throughout this period. After this time, the heating mantle was removed, and while the reaction was still hot, 50 mL of acetone was added, and the resultant solution was stirred at room temperature for an additional $^1/_2$ h. Filtering yielded a dark violet-black microcrystalline solid that was washed with 5 mL of cold H_2O and then dried by suction. Yields ranged from 60 to 75% based on starting ruthenium.

The salts $[(bpy)_2(PnR_3)Ru(II)(Cl)](ClO_4)$ (PnR_3 = tertiary phosphine, arsine, or stibine) were prepared by modifications of published procedures[15] that are outlined below.

$[(bpy)_2(PnR_3)Ru^{II}(Cl)](ClO_4)$ (PnR_3 = PPh_3, $AsPh_3$, $SbPh_3$). *cis*-$Ru(bpy)_2Cl_2 \cdot 2H_2O$ (521 mg, 1 mmol) and 1 mmol of the ligand were added to 100 mL of a nitrogen-deaerated ethanol–water mixture (80% ethanol, 20% water). The mixture was stirred magnetically and heated at reflux for 4–6 h. After this time, the solution was reduced by dryness with a rotary evaporator, and ca. 50 mL of water was then added to the reaction vessel. The complex was precipitated as the perchlorate salt by adding 2 mL of 70% perchloric acid or an excess of sodium perchlorate. The red-orange solid was collected by filtration, washed copiously with water, and air-dried. Purification was achieved through column chromatography on alumina by utilizing toluene–acetonitrile (60:40 by volume) as eluent. The first band was the red-orange complex followed by a second smaller yellow band that was characterized as the disubstitution product. The desired product was purified further by removing the eluent, followed by dissolution in acetone and reprecipitation with ether which generally resulted in microcrystalline solid. Yields were 60–80% (based on ruthenium) of analytically pure product for all salts.

$[(bpy)_2(PR_3)Ru^{II}(Cl)](ClO_4)$ (R = Me, Et, *n*-Pr, *i*-Pr, *n*-Bu, Cy, Bz, *p*-$CF_3C_6H_4$). The same procedure was followed as described for the triaryl–group 5 complexes except longer reaction times (8 h) were necessary to obtain reasonable yields. Chromatography with 1:1 acetonitrile:toluene generally gave a fast-moving violet band that was characterized as the *cis*-$Ru(bpy)_2Cl_2 \cdot 2H_2O$ starting material followed by the red-brown complex, which in turn was followed by a small yellow band that was characterized, in some cases, as the diphosphine complex. Yields varied but averaged 65% (based on Ru) of analytically pure product.

$[(bpy)_2(PR_3)Ru^{II}(OH_2)](ClO_4)_2$ (R = Me, Et, *n*-Pr, *i*-Pr, *n*-Bu). In a typical preparation, 200 mg of $[(bpy)_2(PR_3)Ru^{II}(Cl)](ClO_4)$ and 1.2 equiv of $AgClO_4$ were added together in ca. 150 mL of H_2O. The solution was purged with nitrogen and then heated at reflux for 1 h during which time the solution changed from a red brown cloudy mixture to a red clear solution containing a white precipitate (AgCl). $[(bpy)_2(PR_3)Ru^{II}(Cl)](ClO_4)$ was only slightly soluble initially, but all material went into solution with heating. After the solution was cooled to room temperature, AgCl was filtered off, and the filtrate was then put onto a column of Sephadex SP-C25 ion exchange resin. A 0.05 M $NaClO_4$ solution was initially added to elute a small yellow-colored band containing unreacted starting material, and 0.08 → 0.2 M $NaClO_4$ solutions were then used to elute the desired complex (red band). A small orange-brown band, probably consisting of higher charged materials, re-

(7) McAuliffe, C. A.; Levason, W. *Phosphine, Arsine and Stibene Complexes of the Transition Elements*; Elsevier: Amsterdam, 1979.
(8) Mason, R.; Meek, D. W. *Angew. Chem., Int. Ed. Engl.* **1978**, *17*, 183–194.
(9) Tolman, C. A. *Chem. Rev.* **1977**, *77*, 313–348.
(10) Chatt, J. *Adv. Organomet. Chem.* **1974**, *12*, 1–29.
(11) Emsley, J.; Hall, D. *The Chemistry of Phosphorus*; Harper and Row: London, 1976.
(12) Abbreviations used in this text include the following: Me = methyl; Et = ethyl; *n*-Pr = *n*-propyl; *i*-Pr = isopropyl; *n*-Bu = *n*-butyl; Cy = cyclohexyl; Ph = phenyl; Bz = benzyl.
(13) (a) Marmion, M. E.; Takeuchi, K. J. *J. Coord. Chem.*, submitted for publication. (b) Marmion, M. E.; Takeuchi, K. J. *J. Chem. Soc., Chem. Commun.* **1987**, 1396–1397. (c) Leising, R. A.; Grzybowski, J. J.; Takeuchi, K. J. *Inorg. Chem.*, in press.
(14) Sawyer, D. T.; Roberts, J. L. *Experimental Electrochemistry for Chemists*; John Wiley and Sons: New York, 1974; p 212.
(15) Sullivan, B. P.; Salmon, D. J.; Meyer, T. J. *Inorg. Chem.* **1978**, *17*, 3334–3341.

Scheme I

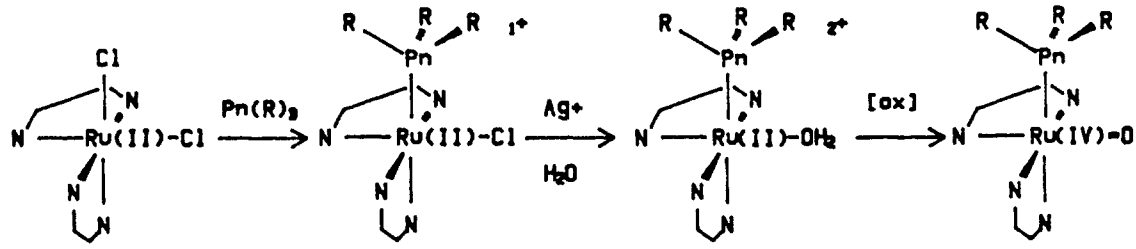

mained at the top of the column. Addition of either $NaClO_4$ or 70% $HClO_4$ to the eluent containing the product caused the precipitation of an orange or red powder which was filtered by suction, washed with cold distilled water, and air-dried. Dark red crystals could be grown when the solid was dissolved in a minimum amount of 0.1 M $NaClO_4$ solution and allowed to stand in the refrigerator 2–3 days. Yields ranged from 70 to 90% of analytically pure product.

$[(bpy)_2(PnR_3)Ru^{II}(OH_2)](ClO_4)_2$ (PnR_3 = PPh_3, $AsPh_3$, PCy_3, PBz_3, $P(p\text{-}CF_3C_6H_4)_3$). In a routine preparation, 150 mg of $[(bpy)_2(PnR_3)Ru^{II}(Cl)](ClO_4)$ and 1.2 equiv of $AgClO_4$ were added to 300 mL of H_2O. The mixture was deaerated with nitrogen and then heated to reflux for 1.5 h. Initially, the ruthenium starting material was insoluble but dissolved in the water with heating. After the solution was cooled to room temperature, AgCl was filtered off, and the filtrate was chilled to precipitate any unreacted starting material which was removed by gravity filtration. The product was precipitated by the addition of 2 mL of 70% $HClO_4$, and the light orange powder was filtered, washed with cold water, and air-dried. Yields ranged from 65 to 75% of analytically pure product.

$[(bpy)_2(SbPh_3)Ru^{II}(NO_2)](ClO_4)$. $[Ru(bpy)_2(NO)(NO_2)](ClO_4)_2$ (250 mg, 0.363 mmol), which was prepared following a literature procedure,[16] and 385 mg (1.09 mmol) of $SbPh_3$ were dissolved in 100 mL of acetone, and the resultant mixture was deaerated with nitrogen. NaN_3 (23.6 mg, 0.363 mmol) was dissolved in the minimum amount of warm methanol (1 mL) and slowly added dropwise to the stirring acetone solution which was continuously purged with N_2. The initial orange solution turned deep red with the addition of azide. The volume was reduced to ~15 mL and then added to 60 mL of stirring ether to precipitate a red-orange solid which was collected by filtration, washed with ether, and air-dried. A yield of 320 mg of crude product was obtained, which was purified by reprecipitation from acetone–ether which yielded 210 mg (63%) of analytically pure product.

$[(bpy)_2(SbPh_3)Ru^{II}(NO)](ClO_4)_3$. $[(bpy)_2(SbPh_3)Ru(NO_2)](ClO_4)$ (200 mg, 0.219 mmol) was suspended in ~100 mL of methanol with vigorous stirring. The initial orange solid changed to a pale yellow with the addition of 70% $HClO_4$, which was added dropwise until the color stopped changing (~1–2 mL). The solid was collected by filtration, wahsed with ether, and air-dried. Purification was achieved through reprecipitation with acetone–ether to obtain a 90% yield of analytically pure product.

$[(bpy)_2(SbPh_3)Ru^{II}(OH_2)](ClO_4)_2$. $[(bpy)_2(SbPh_3)Ru(NO)](ClO_4)_3$ (75 mg, 0.069 mmol) was dissolved in 100 mL of H_2O, and an equimolar amount of NaN_3 (4.5 mg dissolved in a minimum amount of hot methanol) was added dropwise to the stirring solution, and after 1–2 min, the solution color changed from yellow to orange/red. The reaction vessel was then placed in an ice bath, and while the solution was stirring, a saturated $NaClO_4$ solution was added dropwise until an orange precipitate formed. The solid was filtered by suction, washed with cold water, and air-dried; yield 36 mg (53%) of analytically pure product.

$[(bpy)_2(PR_3)Ru^{IV}(O)](ClO_4)_2$ (R = Me, Et, *i*-Pr). $[(bpy)_2(PR_3)Ru^{II}(OH_2)](ClO_4)_2$ (50 mg) was dissolved in a minimum amount of H_2O (ca. 30 mL). The reaction vessel was protected from light and placed in an ice bath to cool. A 20-fold excess of Ce(IV) solution (0.5 N in 6 N $HClO_4$) was added slowly dropwise while the mixture was stirred magnetically at ice temperatures. The initial clear red-orange solution turned pale yellow, and after ca. 1 min, a golden yellow product precipitated which was collected by filtration, washed with cold H_2O, and air-dried. Yields averaged 85–90% of analytically pure product.

$[(bpy)_2(PnR_3)Ru^{IV}(O)(ClO_4)_2$ (PnR_3 = PPh_3, $AsPh_3$, PCy_3, PBz_3). $[(bpy)_2(PnR_3)Ru^{II}(OH_2)](ClO_4)_2$ (50 mg) was dissolved in a minimum amount of water (ca. 60–70 mL). A tenfold excess of Ce(IV) solution (0.5 N in 6 N $HClO_4$) was added slowly dropwise while the mixture was stirred magnetically at room temperature, and during this time, the solution changed from orange to yellow. Yellow solid precipitated within a few seconds of the final addition of cerium. The solid was collected by filtration, wahsed with cold distilled water, and air-dried. Yields generally ranged from 75 to 85% of analytically pure product.

$[(bpy)_2(PEt_3)Ru^{III}(OH)](ClO_4)_2$. $[(bpy)_2(PEt_3)Ru^{II}(OH_2)](ClO_4)_2$ (10.8 mg, 0.0144 mmol) was dissolved in ca. 3 mL of an aqueous solution buffered at pH 6.8 (KH_2PO_4/$NaHPO_4$). The solution was oxidized electrochemically in the absence of light at 0.65 V vs SSCE with a retriculated vitreous carbon working electrode. Electrolysis was carried out until an n = 1 value was reached (ca. 40 min). The reaction vessel was then placed in an ice bath and a saturated $NaClO_4$ solution was added dropwise until precipitation occurred. The yellow-brown solid was filtered by suction, washed with 5 drops of cold H_2O, and air-dried. Yield = 9.5 mg.

$[(bpy)_2(PEt_3)Ru^{IV}(^{18}O)](ClO_4)_2$. $[(bpy)_2(PEt_3)Ru^{II}(OH_2)](ClO_4)_2$ (20 mg) was slurried in 1.5 mL of $H_2{}^{18}O$ (90.97% ^{18}O, 3.49% ^{17}O, 5.54% ^{16}O), obtained from Alfa Products (Morton Thiokol, Inc.), for 1 h. The $H_2{}^{18}O$ was then distilled off by utilizing a static vacuum. The remaining solid was suspended in 0.5 mL of H_2O, the reaction vessel was placed in an ice bath, and a tenfold molar excess of 0.5 N Ce(IV) in 6 N $HClO_4$ was added dropwise, quickly. The initial red-orange slurry turned a golden yellow color after ca. 1 min of stirring. The mixture was quickly sonicated, filtered, and washed with a few drops of cold water. The solid was then dried in vacuo.

Results and Discussion

Syntheses. $[(bpy)_2(PnR_3)Ru^{IV}(O)](ClO_4)_2$ (PnR_3 = tertiary phosphine or arsine) complexes were prepared by the synthetic route outlined in Scheme I. In this manner, the pnictogen ligand was introduced into the complex when the ruthenium was in a low oxidation state in order to prevent the oxidation of the free group 5 ligand. Then, the oxidations of the Ru^{II}—OH_2 species with Ce(IV) to the corresponding Ru^{IV}=O species were performed in aqueous solution at either ice or room temperatures, in which the product spontaneously precipitated from solution once it was formed.

The use of perchlorate as an anion throughout the syntheses of these complexes was necessary to achieve water solubility, which does not occur with hexafluorophosphate salts, and to prevent counteranion oxidation, which does occur if chloride anions are utilized. Although the perchlorate salts of the aquo complexes are less stable than the corresponding hexafluorophosphate salts, both the $[(bpy)_2(PnR_3)Ru^{II}(OH_2)](ClO_4)_2$ and $[(bpy)_2(PnR_3)Ru^{IV}(O)](ClO_4)_2$ complexes remain stable for a minimum of days if they are stored in the freezer.

It was necessary to synthesize $[(bpy)_2(PR_3)Ru^{IV}(O)](ClO_4)_2$ (R = Me or Et) in the absence of light, for a small amount of impurity, which is evidenced in the cyclic voltammogram of these complexes in buffered aqueous solution, is formed photochemically. The impurity is probably the trans isomer, for its $E_{1/2}$ value is 180 mV lower than the $E_{1/2}$ value of the Ru(III)/(II) couple for the cis complex. Such a difference in redox potentials has been reported as characteristic for cis/trans isomers of other phosphine-containing ruthenium(II) complexes,[17,18] where cis → trans conversion occurs photochemially, apparently by irradiation of the lowest lying d → d transition.[17b]

The stability of the trialkylphosphine–ruthenium(IV)–oxo complexes decreased with increasing number of carbon atoms of the alkyl group, i.e., $P(n\text{-}Bu)_3 < P(n\text{-}Pr)_3 < PEt_3 < PMe_3$. For example, $[(bpy)_2(PMe_3)Ru^{IV}(O)](ClO_4)_2$ is stable in the solid state for months and remains stable in solution at room temperature for days. Conversely, all attempts to isolate $[(bpy)_2(P(n\text{-}Bu)_3)$-

(16) Godwin, J. B.; Meyer, T. J. *Inorg. Chem.* **1971**, *10*, 471–474.

(17) (a) Sullivan, B. P.; Calvert, J. M.; Meyer, T. J. *Inorg. Chem.* **1980**, *19*, 1404–1407. (b) Sullivan, B. P.; Meyer, T. J. *Inorg. Chem.* **1982**, *21*, 1037–1040.

(18) Walsh, J. L.; Durham, B. *Inorg. Chem.* **1982**, *21*, 329–332.

$Ru^{IV}(O)](ClO_4)_2$ proved unsuccessful. Upon addition of Ce(IV) to an aqueous solution of $[(bpy)_2(P(n\text{-}Bu)_3)Ru^{II}(OH_2)]^{2+}$, the orange-colored mixture was observed to turn a very pale yellow color as expected; however, upon isolation of the product, the solid reverted to the aquo starting material as evidenced by UV–vis spectroscopy. Similar results were obtained when different chemical oxidants were employed such as H_2O_2 or Br_2. The addition of $(NH_4)_2Ce(NO_3)_6$, in place of the ceric perchlorate solution, to a non-acidic aqueous solution of $[(bpy)_2(P(n\text{-}Bu)_3)Ru^{II}(OH_2)]^{2+}$ produced a deep green material that has properties consistent with oxo-bridged ruthenium complexes.[19] The $[(bpy)_2(P(n\text{-}Pr)_3)Ru^{IV}(O)](ClO_4)_2$ salt was isolable but was unstable in solution while the solid itself decomposed to the aquo complex over a period of several hours. Notably, the return of the original ruthenium complex suggests that the decomposition pathway does not involve oxidation or loss of the phosphine ligand, nor destruction of the bipyridyl rings, as these pathways would not be expected to be reversible. A possible explanation for the facile reduction of these oxo complexes to their corresponding aquo complexes is that the oxo species may be acting as a water oxidant, since the catalytic oxidation of water with Ru(II)–aquo species that have been oxidized chemically or electrochemically has been reported for similar systems.[20] Water oxidation may also account for the instability of the $[(bpy)_2(P(p\text{-}CF_3C_6H_4)_3)Ru^{IV}(O)]^{2+}$ complex in aqueous solution, because this complex has a high oxidation potential, and attempts at oxidation of the Ru(II)–aquo species yields only aquo starting material. Notably, the unstable $[(bpy)_2(PnR_3)Ru^{IV}(O)](ClO_4)_2$ (PnR_3 = PBz_3 or $SbPh_3$) complexes appear to decompose to Ru(III) dimers, as evidenced from their spectral properties.[19]

Attempts to prepare the $[(bpy)_2(SbPh_3)Ru^{II}(OH_2)](ClO_4)_2$ complex from the corresponding chloro species through the use of silver ion were not successful. After filtering off the white precipitate, which contained both AgCl and $SbPh_3$, the addition of either $NaClO_4$ or $HClO_4$ yielded no precipitate. Spectroscopic and electrochemical characterization of the deep red filtrate are consistent with the presence of $[(bpy)_2Ru^{II}(OH_2)_2]^{2+}$.[4b,21] Thus, a ruthenium–nitrosyl/azide synthetic scheme[22] was utilized to obtain $[(bpy)_2(SbPh_3)Ru^{II}(OH_2)](ClO_4)_2$ in good yields. Notably, the deep diaquo complex was also a byproduct in the synthesis of $[(bpy)_2(AsPh_3)Ru^{IV}(O)](ClO_4)_2$, but to a much lesser extent. This suggests that the ruthenium–group 5 ligand bond strengths decrease in the order P > As > Sb, which is consistent with the observations by Tolman for $Fe(CO)_n(ER_3)_m$ complexes, where E = P, As, Sb, Bi.[9]

Analytical Data. Elemental analyses, listed in Table I (supplementary material), indicate that the compounds are obtained as anhydrous or hydrated salts depending on the coordinated ligands. The $[(bpy)_2(PnR_3)Ru^{II}(Cl)](ClO_4)$ complexes could be dried in vacuo, but the oxo and aquo complexes often decomposed on drying. The hydrates are stable under mild conditions, with the presence of the O–H functional group being indicated by $\nu_{O\text{-}H}$ bands centered at ca. 3500 cm^{-1}; more vigorous drying conditions produced decomposition, as evidenced by a red shift of approximately 70 nm in the visible spectrum of the salts of the aquo and oxo species upon decomposition.

Conductivity Data. Conductivity measurements were made on the $[(bpy)_2(PPh_3)Ru^{II}(OH_2)](ClO_4)_2$ and $[(bpy)_2(PPh_3)Ru^{IV}(O)](ClO_4)_2$ complexes in CH_2Cl_2. The experiments were run basically according to the method outlined by Feltham and Hayter[23] in which 5 different stock solutions of each complex in a range of 5.0×10^{-4} to 2.5×10^{-2} M were measured to determine the slope of $\Lambda_o - \Lambda_e$ vs $(C_e)^{1/2}$ plot. The measured conductances (Ω^{-1} cm^2 mol^{-1}) are 292 for $[(bpy)_2(PPh_3)Ru^{II}(OH_2)](ClO_4)_2$ and 306 for $[(bpy)_2(PPh_3)Ru^{IV}(O)](ClO_4)_2$, which suggests these complexes to be 2:1 electrolytes, since the slope of the $\Lambda_o - \Lambda_e$ vs $C_e^{1/2}$ plot is nearly identical with that of $[(bpy)_3Ru^{II}](ClO_4)_2$ (conductance = 298), which was used as a standard.

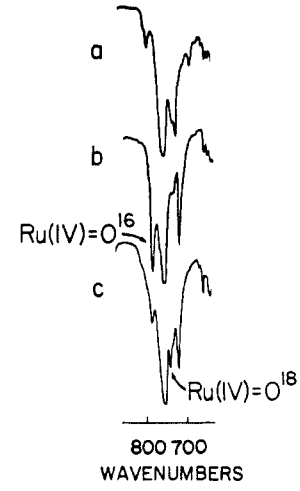

Figure 1. Portion of IR spectra for (a) $[(bpy)_2(PEt_3)Ru^{II}(OH_2)](ClO_4)_2$, (b) $[(bpy)_2(PEt_3)Ru^{II}(^{16}O)](ClO_4)_2$, and (c) $[(bpy)_2(PEt_3)Ru^{II}(^{18}O)](ClO_4)_2$.

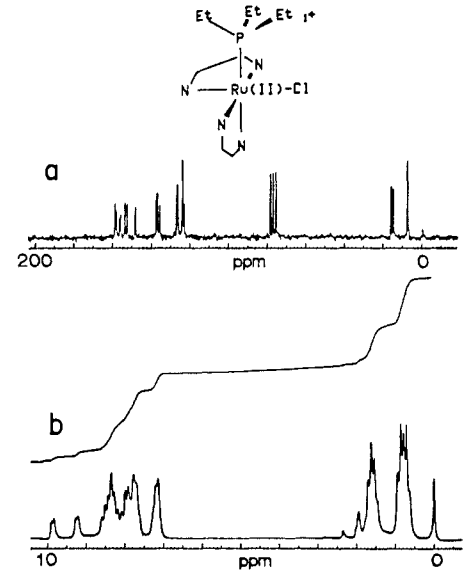

Figure 2. (a) Decoupled ^{13}C NMR spectrum and (b) proton NMR spectrum of 0.1 M $[(bpy)_2(PEt_3)Ru^{II}(Cl)](ClO_4)$ in $CDCl_3$.

IR Spectra. The IR spectra of the $[(bpy)_2(PR_3)Ru^{II}(Cl)](ClO_4)$, $[(bpy)_2(PR_3)Ru^{II}(OH_2)](ClO_4)_2$, and $[(bpy)_2(PR_3)Ru^{IV}(O)](ClO_4)_2$ (R = Me, Et, *i*-Pr) salts in the 4000–600-cm^{-1} region appear very similar, which implies that the $(bpy)_2PR_3Ru$ unit is unaffected throughout the synthesis of the oxo species. However, there is one intense absorbance peak at 790 cm^{-1}, evident only in the $[(bpy)_2(PR_3)Ru^{IV}(O)](ClO_4)_2$ complexes; this peak has been assigned to the Ru^{IV}=O stretch. The peak assignment for the Ru^{IV}=O stretch was confirmed by an isotopic labeling study, where, upon labeling the oxo ligand with ^{18}O, the peak is shifted 40 cm^{-1} and appears at 750 cm^{-1} (Figure 1). This is the expected shift based on a Hooke's law approximation[24] for the Ru^{IV}=O bond. In addition, other reported terminal oxo stretching frequencies for a variety of oxidation states of ruthenium, including

(19) Weaver, T. R.; Meyer, T. J.; Adeyemi, S. A.; Brown, G. M.; Eckberg, R. P.; Hatfield, W. E.; Johnson, E. C.; Murray, R. W.; Vutereker, D. *J. Am. Chem. Soc.* **1975**, *97*, 3039–3049.

(20) For some examples, see: (a) Goswami, S.; Chakravarty, A. R.; Chakravorty, A. *J. Chem. Soc., Chem. Commun.* **1982**, 1288–1289. (b) Honda, K.; Frank, A. *J. Chem. Soc., Chem. Commun.* **1984**, 1635–1636. (c) Gilbert, J. A.; Eggleston, D. S.; Murphy, W. R., Jr.; Geselowitz, D. A.; Gerstein; S. W.; Hodgson, D. J.; Meyer, T. J. *J. Am. Chem. Soc.* **1985**, *107*, 3855–3870.

(21) Griffith, W. P.; Pawson, D. *J. Chem. Soc., Dalton Trans.* **1973**, 1315–1320.

(22) (a) Adeyemi, S. A.; Miller, F. J.; Meyer, T. J. *Inorg. Chem.* **1972**, *11*, 994–999. (b) Durham, B.; Walsh, J. L.; Carter, C. L.; Meyer, T. J. *Inorg. Chem.* **1980**, *19*, 860–865.

(23) Feltham, R. D.; Hayter, R. G. *J. Chem. Soc.* **1964**, 4587–4581.

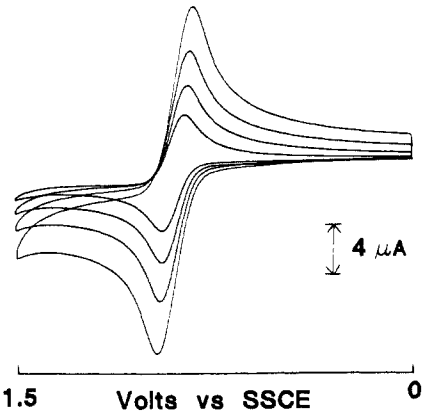

Figure 3. Cyclic voltammograms of $[(bpy)_2(PEt_3)Ru^{II}(Cl)](ClO_4)$ in 0.1 M Bu_4NBF_4/CH_2Cl_2 with a platinum working electrode at scan rates of 50, 100, 200, and 400 mV/s.

Ru(IV), occur in the region 785–890 cm^{-1}.[5,21,25,26]

In the triaryl–pnictogen–ruthenium(IV)–oxo complexes, the Ru^{IV}=O stretches are obscured due to an increase in absorbances in the 800–600-cm^{-1} region. These absorbances are attributed to out-of-plane ring bending vibrations characteristic of aromatic compounds.[24]

NMR Spectra. ^1H and ^{13}C NMR spectroscopies were utilized to determine the ligand arrangement about the ruthenium(II) center for $[(bpy)_2(PEt_3)Ru^{II}(Cl)](ClO_4)$ and $[(bpy)_2(PEt_3)Ru^{II}(OH_2)](ClO_4)_2$. The NMR spectra of both complexes are consistent with a C_1 symmetry for the complexes, which confirms a cis orientation of the chloro/aquo and triethylphosphine ligands. For example, in the ^1H and decoupled ^{13}C spectra of $[(bpy)_2(PEt_3)Ru^{II}(Cl)](ClO_4)$ complex (Figure 2), the complex splitting pattern in the proton NMR in the region from 7 to 10 ppm, and the large number of resonances in the decoupled ^{13}C spectrum in the region from 120 to 160 ppm, arise from the nonequivalence of the individual bipyridine rings when the complex is in the cis configuration. Thus, the 16 resonances in the aromatic region of the decoupled ^{13}C spectra are a result of the 4 slightly dissimilar rings superimposed on one another. The proton NMR of the trans isomers of related bis-bipyridine complexes are characterized by a less complex pattern of resonances from the chelate ring protons as a result of the high symmetry of the bipyridine ligands in the trans conformation.[18]

The cis structural assignments are consistent with most bis-bipyridine transition-metal complexes, where the steric bulk of bipyridine prevents trans orientation of ligands except in several unusual cases.[27] Although the ruthenium(IV)–oxo complexes are paramagnetic and do not produce readily interpretable NMR spectra, the sterically favored cis configuration of the aquo species will most probably be retained in the generation of the oxo species, since the oxidation of Ru(II)–aquo complexes to Ru(IV)–oxo complexes occurs upon mixing and is conducted under mild conditions.

Cyclic Voltammetry. Cyclic voltammetric measurements on 0.1 M tetra-*n*-butylammonium tetrafluoroborate/dichloromethane solutions revealed one reversible couple for all $[(bpy)_2(PnR_3)Ru^{II}(Cl)](ClO_4)$ (PnR_3 = tertiary group 5 ligand) complexes in the range from 0.0 to 2.0 V vs SSCE. As an example of a typical cyclic voltammogram, shown in Figure 3 is the cyclic voltammogram of $[(bpy)_2(PEt_3)Ru^{II}(Cl)](ClO_4)$ in CH_2Cl_2. The half-wave potentials ($E_{1/2}$), obtained from cyclic voltammetry, for each Ru(III)/Ru(II) redox couple from a series of phosphine–ruthenium(II)–chloro complexes are listed in Table II. This one-electron oxidation process is chemically and often electrochemically reversible, as evidenced by the peak current ratios ($i_{p,a}/i_{p,c} \approx 1$) and by a 60-mV separation between the anodic and cathodic peak potentials (ΔE_p). In addition, plots of the peak currents versus the square root of scan velocity at scan rates ≤400 mV/s are linear, which from the Randles-Sevcik equation implies electrochemical reversibility.[28] Notably, $E_{1/2}$ values show a dependence on the pnictogen ligand, where a range of approximately 280 mV can be achieved through R substituent variation on the group 5 ligand.

The redox potentials of the Ru(III)/Ru(II) couple of the corresponding $[(bpy)_2(PnR_3)Ru^{II}(OH_2)](ClO_4)_2$ complexes in CH_2Cl_2 are given in Table III. Cyclic voltammograms of the aquo complexes generally do exhibit scan rate dependence of

Table II. $E_{1/2}$ Potentials for $[(bpy)_2(PnR_3)Ru^{II}Cl]^+$ Complexes in CH_2Cl_2

complex	$E_{1/2}$ (V vs SSCE)
$[(bpy)_2PMe_3Ru^{II}Cl](ClO_4)$	0.92
$[(bpy)_2PEt_3Ru^{II}Cl](ClO_4)$	0.88
$[(bpy)_2P(n\text{-}Pr)_3Ru^{II}Cl](ClO_4)$	0.88
$[(bpy)_2P(i\text{-}Pr)_3Ru^{II}Cl](ClO_4)$	0.87
$[(bpy)_2P(n\text{-}Bu)_3Ru^{II}Cl](ClO_4)$	0.89
$[(bpy)_2PCy_3Ru^{II}Cl](ClO_4)$	0.93
$[(bpy)_2PBz_3Ru^{II}Cl](ClO_4)$	1.00
$[(bpy)_2PPh_3Ru^{II}Cl](ClO_4)$	1.04
$[(bpy)_2AsPh_3Ru^{II}Cl](ClO_4)$	1.01
$[(bpy)_2SbPh_3Ru^{II}Cl](ClO_4)$	1.03
$[(bpy)_2P(p\text{-}CF_3C_6H_4)_3Ru^{II}Cl](ClO_4)$	1.16

Table III. $E_{1/2}$ Potentials for $[(bpy)_2(PnR_3)Ru^{II}OH_2]^{2+}$ Complexes in CH_2Cl_2

complex	$E_{1/2}$ (V vs SSCE)
$[(bpy)_2PMe_3Ru^{II}OH_2](ClO_4)_2$	1.24
$[(bpy)_2PEt_3Ru^{II}OH_2](ClO_4)_2$	1.16
$[(bpy)_2P(n\text{-}Pr)_3Ru^{II}OH_2](ClO_4)_2$	1.18
$[(bpy)_2P(i\text{-}Pr)_3Ru^{II}OH_2](ClO_4)_2$	1.17
$[(bpy)_2P(n\text{-}Bu)_3Ru^{II}OH_2](ClO_4)_2$	1.18
$[(bpy)_2PCy_3Ru^{II}OH_2](ClO_4)_2$	1.22
$[(bpy)_2PBz_3Ru^{II}OH_2](ClO_4)_2$	1.29
$[(bpy)_2PPh_3Ru^{II}OH_2](ClO_4)_2$	1.33
$[(bpy)_2AsPh_3Ru^{II}OH_2](ClO_4)_2$	1.32
$[(bpy)_2SbPh_3Ru^{II}OH_2](ClO_4)_2$	1.39[a]
$[(bpy)_2P(p\text{-}CF_3C_6H_4)_3Ru^{II}OH_2](ClO_4)_2$	1.45[a]

[a] Irreversible, potential cited is the potential of the peak current for a scan rate of 100 mV/s.

Table IV. $E_{1/2}$ Potentials for $[(bpy)_2(PnR_3)Ru^{II}OH_2]^{2+}$ Complexes in Aqueous Solution Buffered at pH 2.00

complex	$E_{1/2}$ (V vs SSCE) Ru^{III}/Ru^{II}	$E_{1/2}$ (V vs SSCE) Ru^{IV}/Ru^{III}
$[(bpy)_2PMe_3Ru^{II}OH_2](ClO_4)_2$	0.79	1.10[a]
$[(bpy)_2PEt_3Ru^{II}OH_2](ClO_4)_2$	0.76	0.97
$[(bpy)_2P(n\text{-}Pr)_3Ru^{II}OH_2](ClO_4)_2$	0.76	0.97
$[(bpy)_2P(i\text{-}Pr)_3Ru^{II}OH_2](ClO_4)_2$	0.75	0.98
$[(bpy)_2P(n\text{-}Bu)_3Ru^{II}OH_2](ClO_4)_2$	0.76	1.02
$[(bpy)_2PCy_3Ru^{II}OH_2](ClO_4)_2$	0.75	0.99
$[(bpy)_2PBz_3Ru^{II}OH_2](ClO_4)_2$	0.78	1.05
$[(bpy)_2PPh_3Ru^{II}OH_2](ClO_4)_2$	0.80	1.06
$[(bpy)_2AsPh_3Ru^{II}OH_2](ClO_4)_2$	0.80	0.97
$[(bpy)_2SbPh_3Ru^{II}OH_2](ClO_4)_2$	0.82[b]	1.10
$[(bpy)_2P(p\text{-}CF_3C_6H_4)_3Ru^{II}OH_2](ClO_4)_2$	1.03[b]	1.23[b]

[a] Redox potentials measured in aqueous solutions buffered at pH 4.0 and 6.8 (based on ~0.059 mV/pH unit), for the couple was too difficult to measure accurately at pH 2.0. [b] Redox couple is irreversible at a scan rate of 100 mV/s; potential cited is $E_{1/2}$ value at 10 mV/s.

(24) Conley, R. T. *Infrared Spectroscopy*, 2nd ed.; Allyn and Bacon: Boston, 1972; p 18.
(25) Griffith, W. P.; Pawson, D. *J. Chem. Soc., Dalton Trans.* **1972**, 1449–1453.
(26) (a) Che, C. M.; Tang, T. W.; Poon, C. K. *J. Chem. Soc., Chem. Commun.* **1984**, 641–642. (b) Che, C. M.; Wong, K. Y.; Poon, C. K. *Inorg. Chem.* **1985**, *24*, 1797–1800. (c) Groves, J. T.; Quinn, R. *Inorg. Chem.* **1984**, *23*, 3844–3846.
(27) For example, see: Durham, B.; Wilson, S. R.; Hodgson, D. J.; Meyer, T. J. *J. Am. Chem. Soc.* **1980**, *102*, 600–607.
(28) Brown, E. R.; Large, R. F. *Physical Methods of Chemistry*; Wiley-Interscience: New York, 1971; Vol. 1, Part IIA, Chapter 6.

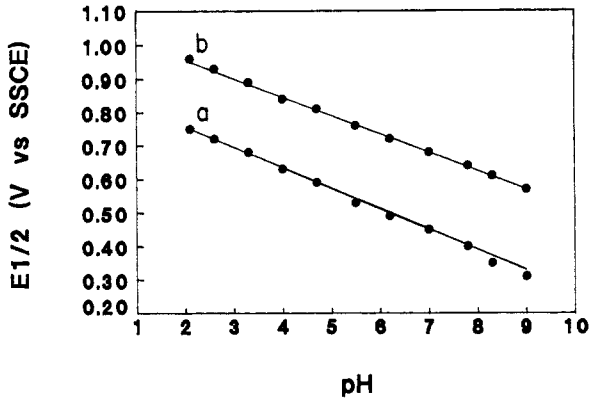

Figure 4. Plots of the observed $E_{1/2}$ values for the $[(bpy)_2(PEt_3)Ru^{II}(OH_2)]^{2+}/[(bpy)_2(PEt_3)Ru^{III}(OH)]^{2+}/[(bpy)_2(PEt_3)Ru^{IV}(O)]^{2+}$ system obtained by cyclic voltammetry as a function of pH.

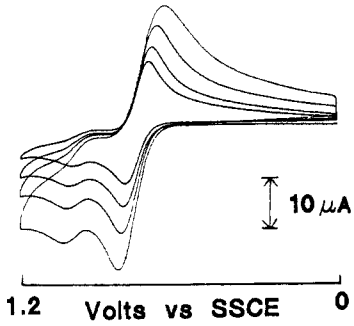

Figure 5. Cyclic voltammograms of $[(bpy)_2(PEt_3)Ru^{II}(OH_2)](ClO_4)_2$ in aqueous solution buffered at pH 2.05 ($NaNO_3/HNO_3$) with a carbon paste working electrode at scan rates of 50, 100, 200, and 400 mV/s.

CH_2Cl_2 solution, with ΔE_p ranging from ~70 mV at a scan rate of 50 mV/s to ~160 mV at a scan rate of 400 mV/s. This is probably due to sluggish electron transfer at the electrode surface. However, in acetonitrile solution, all aquo complexes show reversible Ru(III)/(II) redox couples, which correspond to the substituted CH_3CN complex, $[(bpy)_2(PnR_3)Ru^{II}(CH_3CN)]^{2+}$.

In aqueous buffered solution, the cyclic voltammograms of $[(bpy)_2(PnR_3)Ru^{II}(OH_2)]^{2+}$ (PnR_3 = tertiary pnictogen ligand) complexes display chemically reversible oxidation and reduction waves for two redox couples: $[L_5Ru^{IV}{=}O]^{2+}/[L_5Ru^{III}{-}OH]^{2+}$ and $[L_5Ru^{III}{-}OH]^{2+}/[L_5Ru^{II}{-}OH_2]^{2+}$ (L_5 = two 2,2'-bipyridine ligands and one tertiary group 5 ligand). The redox couples for all aquo complexes measured in aqueous solution buffered at pH 2 are presented in Table IV. The redox potentials for both the Ru(III)/Ru(II) and the Ru(IV)/Ru(III) couples of the representative $[(bpy)_2(PEt_3)Ru^{II}(OH_2)]^{2+}$ complex display potential shifts of −0.061 V per pH unit for Ru(III)/Ru(II) couples and −0.056 V per pH unit for Ru(IV)/Ru(III) couples from solution pH values in the range of 1–9 (Figure 4). This is consistent with one-electron, one-proton transfers based on the Nernstian prediction of −0.059 V/pH unit for a one-electron couple involving the dissociation of one proton:

$$(bpy)_2LRu^{IV}{=}O^{2+} \overset{+H^+,\,+e^-}{\rightleftharpoons} (bpy)_2LRu^{III}{-}OH^{2+} \overset{+H^+,\,+e^-}{\rightleftharpoons} (bpy)_2LRu^{II}{-}OH_2{}^{2+}$$

$$E_{1/2} = +0.72\text{V} \qquad E_{1/2} = +0.46\text{ V}$$

(pH 7, L = PEt_3)

The cyclic voltammograms of $[(bpy)_2(PEt_3)Ru^{II}(OH_2)]^{2+}$ (Figure 5) and $[(bpy)_2PEt_3Ru^{IV}(O)]^{2+}$ (Figure 6) taken in aqueous solution at solution pH values of 1–9 proved to be identical, consistent with the chemically reversible interconversion between $Ru^{IV}{=}O$ and $Ru^{II}{-}OH_2$. Notably, this interconversion is consistent with the structural assignments suggested by the NMR experiments (vide supra), where the cis conformation of the bipyridine ligands in the aquo complexes is retained in the oxo complexes.

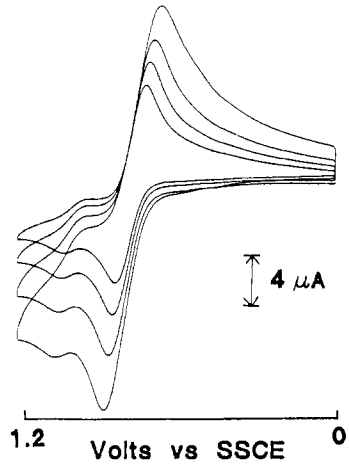

Figure 6. Cyclic voltammograms of $[(bpy)_2(PEt_3)Ru^{IV}(O)](ClO_4)_2$ in aqueous solution buffered at pH 2.05 ($NaNO_3/HNO_3$) with a carbon paste working electrode at scan rates of 50, 100, 200, and 400 mV/s.

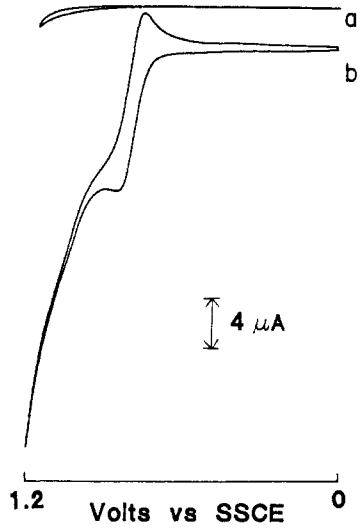

Figure 7. Electrocatalytic oxidation of benzyl alcohol with $[(bpy)_2(PEt_3)Ru^{II}(OH_2)](ClO_4)_2$ as the catalyst. Cyclic voltammograms of (a) 0.12 M benzyl alcohol and (b) 0.12 M benzyl alcohol and 0.0013 M Ru(II) in aqueous solution buffered at pH 2.05 ($NaNO_3/HNO_3$) with a carbon paste working electrode at scan rate of 5 mV/s.

The Ru(III)/Ru(II) couple appears to be well-behaved, whereas the Ru(IV)/Ru(III) couple appears quasi-reversible at best. In fact, the appearance of the second couple is very sensitive to the electrode surface where best results were obtained when a carbon paste electrode was employed, rather than a glassy-carbon electrode. Notably, the Ru(IV)/Ru(III) couple was lost completely in most cases when the glassy-carbon electrode was polished and activated.[29] This intuitively was opposite from what was expected on the basis of improved cyclic voltammograms obtained for the oxidation of catechol when an activated glassy-carbon electrode was used, for catechol oxidation also involves proton-coupled electron transfer.[30] This behavior demonstrates the profound influence of the tertiary phosphine or arsine ligand on the electron transfer properties of the $[(bpy)_2(PEt_3)Ru^{III}(OH)]^{2+}$ complexes.

In further cyclic voltammetric studies, upon addition of excess benzyl alcohol to a dilute aqueous solution of $[(bpy)_2(PEt_3)Ru^{II}(OH_2)]^{2+}$, the potential for the onset of alcohol oxidation becomes less positive (lower overpotential) by 600 mV and appears

(29) The electrodes were polished with 1-μm alumina for 2 min, rinsed with deionized water, and sonicated with a Branson B-12 ultrasonic cleaner in a beaker containing deionized water. The electrodes were activated oxidatively in non-degassed 0.1 M H_2SO_4 for 1 min at an applied potential of 1.80 V vs SSCE.

(30) Murphy, W. R., Jr. Ph.D. Dissertation, University of North Carolina, Chapel Hill, North Carolina, 1978.

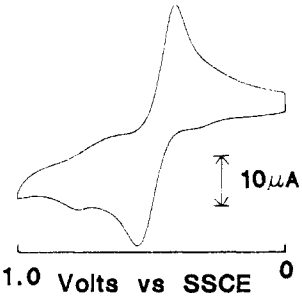

Figure 8. Cyclic voltammogram of $[(bpy)_2(PEt_3)Ru^{III}(OH)](ClO_4)_2$ in aqueous solution buffered at pH 6.8 (KH_2PO_4/Na_2HPO_4) with a glassy carbon working electrode at scan rate 100 mV/s.

Table V. UV–vis Spectral Data of $[(bpy)_2(PnR_3)Ru^{II}Cl]^+$ Complexes in CH_2Cl_2

complex	λ_{max}, nm ($\epsilon_{max} \times 10^{-3}$, M^{-1} cm^{-1})
$[(bpy)_2PMe_3Ru^{II}Cl](ClO_4)$	476 (7.8); 341 (7.3); 290 (47)
$[(bpy)_2PEt_3Ru^{II}Cl](ClO_4)$	486 (7.8); 341 (7.4); 290 (41)
$[(bpy)_2P(n\text{-}Pr)_3Ru^{II}Cl](ClO_4)$	488 (7.6); 346 (7.4); 292 (42)
$[(bpy)_2P(i\text{-}Pr)_3Ru^{II}Cl](ClO_4)$	490 (7.2); 346 (7.1); 294 (39)
$[(bpy)_2P(n\text{-}Bu)_3Ru^{II}Cl](ClO_4)$	486 (7.6); 342 (7.3); 293 (42)
$[(bpy)_2PCy_3Ru^{II}Cl](ClO_4)$	494 (7.7); 348 (7.5); 293 (39)
$[(bpy)_2PBz_3Ru^{II}Cl](ClO_4)$	478 (7.3); 334 (7.4); 289 (38)
$[(bpy)_2PPh_3Ru^{II}Cl](ClO_4)$	461 (7.3); 332 (7.3); 292 (41)
$[(bpy)_2AsPh_3Ru^{II}Cl](ClO_4)$	474 (7.5); 338 (7.5); 292 (42)
$[(bpy)_2SbPh_3Ru^{II}Cl](ClO_4)$	472 (7.7); 338 (7.7); 292 (41)
$[(bpy)_2P(p\text{-}CF_3C_6H_4)_3Ru^{II}Cl](ClO_4)$	448 (7.4); 326 sh (6); 294 (39)

at the redox potential of the Ru(IV)/Ru(III) couple (Figure 7). Thus, since the phosphine–ruthenium(IV)–oxo complex can be generated at moderate potentials in aqueous solution, under suitable conditions, phosphine–ruthenium(II)–aquo complexes can serve as catalysts in electrocatalytic processes.

Coulometry. Controlled potential electrolysis was carried out in the dark on aqueous solutions containing the $[(bpy)_2(PEt_3)Ru^{II}(OH_2)]^{2+}$ complex, buffered at pH 6.86 (KH_2PO_4/Na_2HPO_4) or pH 2.20 ($HClO_4/LiClO_4$), and the products were monitored by cyclic voltammetry and UV–vis spectroscopy. Exhaustive electrolysis past the second wave (0.85 V vs SSCE at pH 6.86) gave an $n = 2$ value, and a UV–vis spectrum of the solution is consistent with the quantitative conversion to $[(bpy)_2(PEt_3)Ru^{IV}(O)]^{2+}$ complex. Then, exhaustive electrolysis at 0.3 V showed that $[(bpy)_2(PEt_3)Ru^{II}(OH_2)]^{2+}$ reforms quantitatively ($n = 2$) as evidenced spectrophotometrically.

If the potential is held past the first wave (0.65 V vs SSCE in pH 6.86) and electrolysis is carried out until $n = 1.0$, a UV–vis spectrum and cyclic voltammogram of the solution are indicative of the $[(bpy)_2(PEt_3)Ru^{III}(OH)]^{2+}$ complex,[5] which can then be isolated with the addition of $NaClO_4$ to the solution. The cyclic voltammogram of the $[(bpy)_2(PEt_3)Ru^{III}(OH)]^{2+}$ complex (Figure 8), taken in aqueous solution, is identical with that of the $[(bpy)_2(PEt_3)Ru^{II}(OH_2)]^{2+}$ complex except for a small amount of impurity, with an $E_{1/2} = 0.30$ V, which is believed to be the trans isomer, for Ru^{II}–phosphine complexes have been found to readily undergo isomerization upon oxidation to Ru(III).[17] The electronic spectrum of the Ru^{III}–OH species shown in Figure 9 [$\lambda_{max} = 384$ nm (ϵ 4000); $\lambda_{max} = 289$ nm (ϵ 28 000); $\lambda_{max} = 245$ nm (ϵ = 20 000); $\lambda_{max} = 205$ nm (ϵ 32 000)] is characteristic of the spectra of other bipyridine complexes of Ru(III) with a hydroxy bound ligand.[5] The small amount of *trans*-Ru^{II}–OH_2 impurity is also observed in the UV–vis spectrum as evidenced by a small peak at $\lambda_{max} = 466$ nm.

Electronic Absorption Spectra. Electronic absorption spectra for the $[(bpy)_2(PnR_3)Ru^{II}Cl]^+$, $[(bpy)_2(PnR_3)Ru^{II}(OH_2)]^{2+}$, and $[(bpy)_2(PnR_3)Ru^{IV}(O)]^{2+}$ complexes were obtained in a number of different solvents in order to quantitatively investigate the reactivity of the oxo complexes under various solvent conditions, and the spectral data for all complexes studied are summarized in Tables V, VI, and VII.

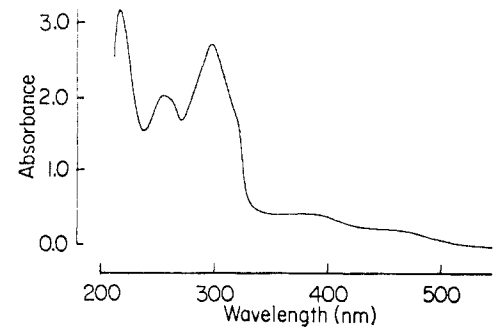

Figure 9. Electronic spectrum of $[(bpy)_2(PEt_3)Ru^{III}(OH)](ClO_4)_2$ (6.4×10^{-5} M) in aqueous solution buffered at pH 6.8 (KH_2PO_4/Na_2HPO_4).

Table VI. UV–vis Spectral Data of $[(bpy)_2(PnR_3)Ru^{II}OH_2]^{2+}$ and $[(bpy)_2(PnR_3)Ru^{IV}(O)]^{2+}$ Complexes in CH_3CN and CH_2Cl_2

complex	λ_{max}, nm ($\epsilon_{max} \times 10^{-3}$, M^{-1} cm^{-1})	solvent
$[(bpy)_2PMe_3Ru^{II}OH_2](ClO_4)_2$	445 (7.3); 328 sh (7); 286 (43)	CH_2Cl_2
$[(bpy)_2PMe_3Ru^{II}OH_2](ClO_4)_2$	428 (7.0); 285 (47)	CH_3CN
$[(bpy)_2PMe_3Ru^{IV}(O)](ClO_4)_2$	300 (20)	CH_2Cl_2
$[(bpy)_2PMe_3Ru^{IV}(O)](ClO_4)_2$	298 (21)	CH_3CN
$[(bpy)_2PEt_3Ru^{II}OH_2](ClO_4)_2$	454 (7.1); 331 sh (7); 286 (43)	CH_2Cl_2
$[(bpy)_2PEt_3Ru^{II}OH_2](ClO_4)_2$	425 (7.2); 284 (47)	CH_3CN
$[(bpy)_2PEt_3Ru^{IV}(O)](ClO_4)_2$	300 (21)	CH_2Cl_2
$[(bpy)_2PEt_3Ru^{IV}(O)](ClO_4)_2$	300 (23)	CH_3CN
$[(bpy)_2P(n\text{-}Pr)_3Ru^{II}OH_2](ClO_4)_2$	455 (7.2); 332 sh (7); 289 (43)	CH_2Cl_2
$[(bpy)_2P(n\text{-}Pr)_3Ru^{II}OH_2](ClO_4)_2$	423 (7.3); 284 (45)	CH_3CN
$[(bpy)_2P(i\text{-}Pr)_3Ru^{II}OH_2](ClO_4)_2$	456 (7.0); 330 (7); 287 (45)	CH_2Cl_2
$[(bpy)_2P(i\text{-}Pr)_3Ru^{II}OH_2](ClO_4)_2$	428 (7.2); 284 (44)	CH_3CN
$[(bpy)_2P(i\text{-}Pr)_3Ru^{IV}(O)](ClO_4)_2$	300 (21)	CH_2Cl_2
$[(bpy)_2P(i\text{-}Pr)_3Ru^{IV}(O)](ClO_4)_2$	300 (23)	CH_3CN
$[(bpy)_2P(n\text{-}Bu)_3Ru^{II}OH_2](ClO_4)_2$	454 (7.2); 331 (7); 288 (43)	CH_2Cl_2
$[(bpy)_2P(n\text{-}Bu)_3Ru^{II}OH_2](ClO_4)_2$	425 (7.2); 283 (46)	CH_3CN
$[(bpy)_2PCy_3Ru^{II}OH_2](ClO_4)_2$	449 (7.3); 330 (7); 288 (43)	CH_2Cl_2
$[(bpy)_2PCy_3Ru^{II}OH_2](ClO_4)_2$	427 (7.0); 286 (45)	CH_3CN
$[(bpy)_2PCy_3Ru^{IV}(O)](ClO_4)_2$	299 (23)	CH_2Cl_2
$[(bpy)_2PCy_3Ru^{IV}(O)](ClO_4)_2$	299 (22)	CH_3CN
$[(bpy)_2PBz_3Ru^{II}OH_2](ClO_4)_2$	439 (7.1); 287 (41)	CH_2Cl_2
$[(bpy)_2PBz_3Ru^{II}OH_2](ClO_4)_2$	415 (7.2); 285 (40)	CH_3CN
$[(bpy)_2PPh_3Ru^{II}OH_2](ClO_4)_2$	438 (7.1); 289 (43)	CH_2Cl_2
$[(bpy)_2PPh_3Ru^{II}OH_2](ClO_4)_2$	405 (7.1); 283 (38)	CH_3CN
$[(bpy)_2PPh_3Ru^{IV}(O)](ClO_4)_2$	300 (22)	CH_2Cl_2
$[(bpy)_2PPh_3Ru^{IV}(O)](ClO_4)_2$	300 (22)	CH_3CN
$[(bpy)_2AsPh_3Ru^{II}OH_2](ClO_4)_2$	439 (7.2); 289 (40)	CH_2Cl_2
$[(bpy)_2AsPh_3Ru^{II}OH_2](ClO_4)_2$	416 (7.0); 289 (41)	CH_3CN
$[(bpy)_2AsPh_3Ru^{IV}(O)](ClO_4)_2$	300 (22)	CH_2Cl_2
$[(bpy)_2AsPh_3Ru^{IV}(O)](ClO_4)_2$	300 (22)	CH_3CN
$[(bpy)_2SbPh_3Ru^{II}OH_2](ClO_4)_2$	443 (7.0); 287 (40)	CH_2Cl_2
$[(bpy)_2SbPh_3Ru^{II}OH_2](ClO_4)_2$	419 (7.0); 282 (39)	CH_3CN
$[(bpy)_2P(p\text{-}CF_3C_6H_4)_3Ru^{II}OH_2](ClO_4)_2$	443 (7.0); 287 (40)	CH_2Cl_2
$[(bpy)_2P(p\text{-}CF_3C_6H_4)_3Ru^{II}OH_2](ClO_4)_2$	391 (7.2); 287 (38)	CH_3CN

Table VII. UV–vis Spectral Data of $[(bpy)_2(PnR_3)Ru^{II}OH_2]^{2+}$ and $[(bpy)_2(PnR_3)Ru^{IV}(O)]^{2+}$ Complexes in H_2O[a]

complex	λ_{max}, nm ($\epsilon_{max} \times 10^{-3}$, M^{-1} cm^{-1})
$[(bpy)_2PMe_3Ru^{II}OH_2](ClO_4)_2$	443 (7.0); 285 (38)
$[(bpy)_2PMe_3Ru^{IV}(O)](ClO_4)_2$	301 (21)
$[(bpy)_2PEt_3Ru^{II}OH_2](ClO_4)_2$	450 (7.6); 287 (39)
$[(bpy)_2PEt_3Ru^{IV}(O)](ClO_4)_2$	299 (20)
$[(bpy)_2P(n\text{-}Pr)_3Ru^{II}OH_2](ClO_4)_2$	452 (7.5); 287 (39)
$[(bpy)_2P(i\text{-}Pr)_3Ru^{II}OH_2](ClO_4)_2$	450 (7.6); 286 (41)
$[(bpy)_2P(i\text{-}Pr)_3Ru^{IV}(O)](ClO_4)_2$	298 (22)
$[(bpy)_2P(n\text{-}Bu)_3Ru^{II}OH_2](ClO_4)_2$	450 (7.6); 287 (41)
$[(bpy)_2PCy_3Ru^{II}OH_2](ClO_4)_2$	443 (7.2); 286 (39)
$[(bpy)_2PCy_3Ru^{IV}(O)](ClO_4)_2$	299 (21)
$[(bpy)_2PBz_3Ru^{II}OH_2](ClO_4)_2$	429 (7.5); 287 (39)
$[(bpy)_2PPh_3Ru^{II}OH_2](ClO_4)_2$	427 (7.7); 287 (39)
$[(bpy)_2PPh_3Ru^{IV}(O)](ClO_4)_2$	300 (21)
$[(bpy)_2AsPh_3Ru^{II}OH_2](ClO_4)_2$	429 (7.6); 287 (39)
$[(bpy)_2AsPh_3Ru^{IV}(O)](ClO_4)_2$	300 (22)
$[(bpy)_2SbPh_3Ru^{II}OH_2](ClO_4)_2$	430 (7.7); 287 (39)
$[(bpy)_2P(p\text{-}CF_3C_6H_4)_3Ru^{II}OH_2](ClO_4)_2$	412 (7.4); 287 (39)

[a] In pH 2.00 ($NaNO_3/HNO_3$ buffer; $\mu = 0.063$). ϵ values for $\pi \rightarrow \pi^*$ transitions were calculated by subtracting out the absorbance due to the nitrate buffer.

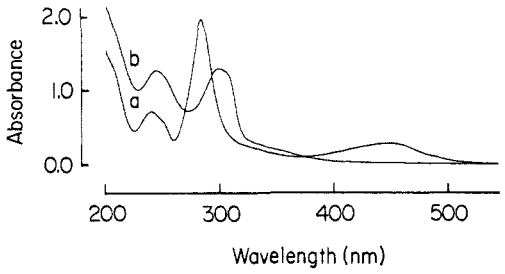

Figure 10. Electronic spectra of (a) $[(bpy)_2(PEt_3)Ru^{II}(OH_2)](ClO_4)_2$ (4.0×10^{-5} M) and (b) $[(bpy)_2(PEt_3)Ru^{IV}(O)](ClO_4)_2$ (8.0×10^{-5} M) in H_2O.

$[(bpy)_2(PnR_3)Ru^{II}(Cl)]^+$ complexes in CH_2Cl_2 exhibit three absorptions in the range from 750 to 250 nm,[15] where the position of the lowest energy absorption maximum depends on the electronic nature of the group 5 ligand. This long-wavelength band can be attributed to a metal-to-ligand $d\pi$ (Ru) $\rightarrow \pi^*$ (bpy) charge transfer (MLCT) transition, consistent with typical bis-(2,2′-bipyridine)ruthenium(II) complexes.[31] In general, there is a linear correlation between the maxima of this MLCT absorption and the $E_{1/2}$ of the Ru(III)/Ru(II) couple for all the chloro complexes. This observation implies that the LUMO involved in the MLCT absorption process is the same orbital involved in the first electrochemical reduction and that the energy of this π^* bipyridine-localized orbital is generally unaffected by variation of substituents on the group 5 ligand.[32,33] The band with a λ_{max} centered about 340 nm is assigned to another MLCT transition, probably $d\pi$ (Ru) $\rightarrow \pi_2^*$ (bpy), due to both the energy of the absorbance as well as the extinction coefficient value.[15] The intense band centered at 290 nm can be assigned to $\pi \rightarrow \pi^*$ ligand-localized transitions of bipyridine which are also characteristic of related complexes.[31]

The spectral features of the $[(bpy)_2(PnR_3)Ru^{II}(OH_2)]^{2+}$ complexes also include an intense visible absorption band assigned to a MLCT transition, a charge transfer band centered at λ_{max} = 330 nm, and a very intense band in the Uv assigned to $\pi \rightarrow \pi^*$ excitation. In general, the bands are shifted to higher energies for the dicationic aquo complexes compared to the corresponding chloro species, probably due to an increased formal charge on the ruthenium ion, thus stabilizing the $d\pi$ (Ru) orbitals. In complexes that contain phosphines that are weaker σ donors or stronger π acids, i.e., where PnR_3 = PPh_3, $AsPh_3$, $SbPh_3$, PBz_3, $P(p\text{-}CF_3C_6H_4)_3$, the two charge transfer (CT) bands move to higher energies such that the higher energy CT transition is obscured by the $\pi \rightarrow \pi^*$ transition localized on the bipyridine ligand.

The rapid formation of $[(bpy)_2(PnR_3)Ru^{II}(CH_3CN)]^{2+}$ upon dissolving $[(bpy)_2(PnR_3)Ru^{II}(OH_2)](ClO_4)_2$ in CH_3CN was evidenced spectrophotometrically where no time dependence of the spectra was detected, indicating that substitution occurred essentially on mixing. Thus, extinction coefficients were calculated on the basis of the CH_3CN substituted complex (Table VI).

All $[(bpy)_2(PnR_3)Ru^{IV}(O)]^{2+}$ complexes characteristically display no visible spectral features, and one $\pi \rightarrow \pi^*$ transition in the UV region with a λ_{max} = 300 nm and an extinction coefficient that is approximately $^1/_2$ of the extinction coefficient of the analogous Ru^{II}–aquo complexes. Since the UV–vis spectra of the $[(bpy)_2(PnR_3)Ru^{II}(OH_2)]^{2+}$ and $[(bpy)_2(PnR_3)Ru^{IV}(O)]^{2+}$ complexes are significantly different (see Tables VI and VII), any oxidation reaction where the Ru^{IV}=O species is reduced to the Ru^{II}–OH_2 species can be monitored spectrophotometrically, by observing the growth of the MLCT transition for the Ru(II)–aquo complex present in the visible region of the spectra (Figure 10).

Reactivity. $[(bpy)_2(PnR_3)Ru^{IV}(O)]^{2+}$ complexes oxidize a number of organic and inorganic substrates, including alcohols to aldehydes and ketones, aldehydes to acids, free phosphines to phosphine oxides, sulfides to sulfoxides, sulfoxides to sulfones, and olefins to epoxides or their corresponding allylic oxidation products.[13] The oxidation of substrates by $[(bpy)_2(PnR_3)Ru^{IV}(O)]^{2+}$ (PnR_3 = PEt_3, PPh_3, $P(i\text{-}Pr)_3$, PCy_3, $AsPh_3$) complexes proceeds very smoothly by second-order kinetics, first order in both ruthenium and substrate. For example, the oxidation of benzyl alcohol by $[(bpy)_2(PPh_3)Ru^{IV}(O)]^{2+}$ displays clean spectral changes from Ru^{IV}=O to Ru^{II}–OH_2, where all intermediate spectra are isosbestic in nature, corresponding to a mixture of only the Ru(IV) and Ru(II) species (Figure 11). Such well-defined, cleanly second order kinetics are a result of the inhibition of $[(bpy)_2(PnR_3)Ru^{III}(OH)]^{2+}$ (PnR_3 = PEt_3, PPh_3, $P(i\text{-}Pr)_3$, PCy_3, $AsPh_3$) formation. The conproportionation of Ru(IV) and Ru(II) complexes generating the corresponding Ru(III) has generally been observed for polypyridyl-based complexes,[34] which results in complicated and less specific substrate oxidation mechanisms.[35] The very slow conproportionation between $[(bpy)_2(PnR_3)Ru^{II}(OH_2)]^{2+}$ and $[(bpy)_2(PnR_3)Ru^{IV}(O)]^{2+}$ (PnR_3 = PEt_3, PPh_3, $P(i\text{-}Pr)_3$, PCy_3, $AsPh_3$) complexes can be attributed to the steric bulk of the pnictogen ligand, where the close approach of the Ru^{IV}=O moiety to the Ru^{II}—OH_2 site, in order to effect hydrogen atom transfer,[34] is slowed appreciably. This is supported by the observation that only a mixture of $[(bpy)_2(PMe_3)Ru^{IV}(O)]^{2+}$ and $[(bpy)_2(PMe_3)Ru^{II}(OH_2)]^{2+}$ rapidly results in conproportionation to $[(bpy)_2(PMe_3)Ru^{III}(OH)]^{2+}$, where trimethylphosphine is the most sterically unhindered tertiary phosphine ligand. In addition, the conproportionation reaction between a Ru(IV) and a Ru(II) species is anticipated thermodynamically for the trimethylphosphine species, for the difference (310 mV) between the potential value of the $[(bpy)_2(PMe_3)Ru^{IV}(O)]^{2+}/[(bpy)_2(PMe_3)Ru^{III}(OH)]^{2+}$ couple and the potential value of the $[(bpy)_2(PMe_3)Ru^{III}(OH)]^{2+}/[(bpy)_2(PMe_3)Ru^{II}(OH_2)]^{2+}$ couple, as

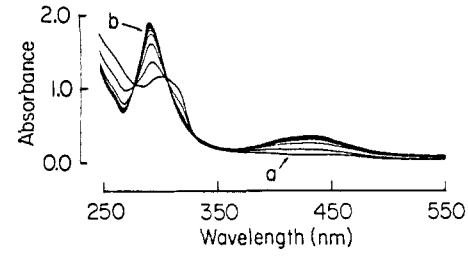

Figure 11. Spectral changes observed in the reaction of benzyl alcohol, 0.03 M, with $[(bpy)_2(PPh_3)Ru^{IV}(O)](ClO_4)_2$ (5.0×10^{-5} M) in aqueous solution buffered at pH 2.05 ($NaNO_3/HNO_3$). Spectra were recorded at 6-min intervals. Spectrum a is the initial spectrum of $[(bpy)_2(PPh_3)Ru^{IV}(O)](ClO_4)_2$, prior to the addition of alcohol (time = 0), and spectrum b is the final spectrum at the time = 42 min, which represents the quantitative conversion to $[(bpy)_2PPh_3Ru^{II}(OH_2)](ClO_4)_2$ at the completion of the reaction.

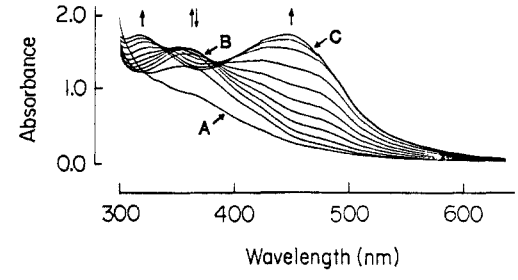

Figure 12. Spectral changes observed in the oxidation of 2-propanol (0.05 M) by $[(bpy)_2(PMe_3)Ru^{IV}(O)](ClO_4)_2$ (2.5×10^{-4} M) in CH_2Cl_2 after (A) 0, (B) 24, and (C) 66 min. Spectrum B is consistent with a Ru^{III}–OH species.

(31) Bryant, G. M.; Fergusson, J. E.; Powell, H. K. J. *Aust. J. Chem.* **1971**, *24*, 257–286.
(32) DeArmond, M. K.; Carlin, C. M. *Coord. Chem. Rev.* **1981**, *36*, 325–355.
(33) Vlcek, A. A. *Coord. Chem. Rev.* **1982**, *43*, 39–62.
(34) Binstead, R. A.; Moyer, B. A.; Samuels, G. J.; Meyer, T. J. *J. Am. Chem. Soc.* **1981**, *103*, 2897–2899.
(35) For example, see: (a) Roecker, L.; Meyer, T. J. *J. Am. Chem. Soc.* **1986**, *108*, 4066–4073. (b) Benson, D. *Mechanisms of Oxidation by Metal Ions*; Elsevier: New York, 1976; Monograph 10. (c) Sheldon, R. A.; Kochi, J. K. *Metal-Catalyzed Oxidations of Organic Compounds*; Academic: New York, 1981.

measured by cyclic voltammetry, is the largest for all of the complexes listed in Table IV. Thus, from the spectral changes observed in the oxidation of an alcohol by $[(bpy)_2(PMe_3)Ru^{IV}(O)]^{2+}$ (Figure 12), the kinetics of substrate oxidation are complicated, because a Ru^{III}–OH intermediate is observed and can function as a one-electron oxidant, independent of the Ru^{IV}=O oxidation chemistry.

Conclusion

The synthetic chemistry of ruthenium(II) complexes which utilize bipyridine and pnictogen ligands has been developed in the systematic preparation of a variety of $[(bpy)_2(PnR_3)Ru^{II}(OH_2)](ClO_4)_2$ complexes, which can be oxidized under mild conditions to the analogous ruthenium(IV)–oxo complexes. These syntheses demonstrate that, under appropriate conditions, easily oxidized pinctogen ligands remain *intact* in the coordination sphere of a potent oxidizing metal center, such as ruthenium(IV)–oxo, to generate fundamentally new ruthenium complexes. Thus, pinctogen ligands can now be used to control the redox potentials of the available ruthenium-centered redox couples, to solubilize the ruthenium(IV)–oxo complexes in both polar and less polar solvents, to kinetically limit the formation of ruthenium(III) from ruthenium(II) and ruthenium(IV), and to exert unusual ligand properties, such as hydrophobic effects or catalytic properties, on the substrate oxidation chemistry of the ruthenium(IV)–oxo moiety.

Acknowledgment. This work was supported in part by the donors of the Petroleum Research Fund, administered by the American Chemical Society, the Cottrell Research Corportion, and both the Biomedical Research Support Grant and the Research Development Fund of SUNY at Buffalo. In addition, the authors gratefully acknowledge the contributions of Stephen A. Kubow to this paper.

Registry No. *cis*-$Ru^{II}(bpy)_2Cl_2$, 19542-80-4; *cis*-$[(bpy)_2PMe_3Ru^{II}Cl](ClO_4)$, 112088-07-0; *cis*-$[(bpy)_2PEt_3Ru^{II}Cl](ClO_4)$, 99687-22-6; *cis*-$[(bpy)_2P(n\text{-}Pr)_3Ru^{II}Cl](ClO_4)$, 112088-09-2; *cis*-$[(bpy)_2P(i\text{-}Pr)_3Ru^{II}Cl](ClO_4)$, 112088-11-6; *cis*-$[(bpy)_2P(n\text{-}Bu)_3Ru^{II}Cl](ClO_4)$, 112088-12-7; *cis*-$[(bpy)_2PCy_3Ru^{II}Cl](ClO_4)$, 112088-14-9; *cis*-$[(bpy)_2PBz_3Ru^{II}Cl](ClO_4)$, 112088-16-1; *cis*-$[(bpy)_2PPh_3Ru^{II}Cl](ClO_4)$, 112088-17-2; *cis*-$[(bpy)_2AsPh_3Ru^{II}Cl](ClO_4)$, 103727-05-5; *cis*-$[(bpy)_2SbPh_3Ru^{II}Cl](ClO_4)$, 112088-18-3; *cis*-$[(bpy)_2P(p\text{-}CF_3C_6H_4)_3Ru^{II}Cl](ClO_4)$, 112088-20-7; *cis*-$[(bpy)_2PMe_3Ru^{II}OH_2](ClO_4)_2$, 112088-22-9; *cis*-$[(bpy)_2PEt_3Ru^{II}OH_2](ClO_4)_2$, 99705-87-0; *cis*-$[(bpy)_2P(n\text{-}Pr)_3Ru^{II}OH_2](ClO_4)_2$, 112112-48-8; *cis*-$[(bpy)_2P(i\text{-}Pr)_3Ru^{II}OH_2](ClO_4)_2$, 112088-24-1; *cis*-$[(bpy)_2P(n\text{-}Bu)_3Ru^{II}OH_2](ClO_4)_2$, 112088-26-3; *cis*-$[(bpy)_2PCy_3Ru^{II}OH_2](ClO_4)_2$, 112088-28-5; *cis*-$[(bpy)_2PBz_3Ru^{II}OH_2](ClO_4)_2$, 112088-30-9; *cis*-$[(bpy)_2PPh_3Ru^{II}OH_2](ClO_4)_2$, 111743-41-0; *cis*-$[(bpy)_2AsPh_3Ru^{II}OH_2](ClO_4)_2$, 112088-32-1; *cis*-$[(bpy)_2SbPh_3Ru^{II}OH_2](ClO_4)_2$, 112088-34-3; *cis*-$[(bpy)_2P(p\text{-}CF_3C_6H_4)_3Ru^{II}OH_2](ClO_4)_2$, 112088-36-5; *cis*-$[(bpy)_2SbPh_3Ru^{II}NO_2](ClO_4)$, 112088-38-7; *cis*-$[Ru(bpy)_2(NO)(NO_2)](ClO_4)_2$, 112088-39-8; *cis*-$[(bpy)_2SbPh_3Ru^{II}(NO)](ClO_4)_3$, 112088-41-2; *cis*-$[(bpy)_2(PMe_3)Ru^{IV}(O)](ClO_4)_2$, 112088-43-4; *cis*-$[(bpy)_2(PEt_3)Ru^{IV}(O)](ClO_4)_2$, 99687-21-5; *cis*-$[(bpy)_2(P\text{-}i\text{-}Pr_3)Ru^{IV}(O)](ClO_4)_2$, 112088-45-6; *cis*-$[(bpy)_2(PPh_3)Ru^{IV}(O)](ClO_4)_2$, 111743-44-3; *cis*-$[(bpy)_2(AsPh_3)Ru^{IV}(O)](ClO_4)_2$, 112088-47-8; *cis*-$[(bpy)_2(PCy_3)Ru^{IV}(O)](ClO_4)_2$, 112088-49-0; *cis*-$[(bpy)_2(PBz_3)Ru^{IV}(O)](ClO_4)_2$, 112088-51-4; *cis*-$[(bpy)_2(PEt_3)Ru^{III}OH](ClO_4)_2$, 112088-52-5; *cis*-$[(bpy)_2(PEt_3)Ru^{IV}(^{18}O)](ClO_4)_2$, 112088-54-7; $RuCl_3$, 10049-08-8.

Supplementary Material Available: Elemental analyses of complexes (Table I) (2 pages). Ordering information is given on any current masthead page.

Molecular Design Based on Inclusion Chemistry. Synthesis, Characterization, and Crystal Structures of a New Family of Lacunar Schiff Base Complexes with Promise as Broad-Range Host Molecules

Dorai Ramprasad, Wang-Kan Lin, Kenneth A. Goldsby, and Daryle H. Busch*

Contribution from the Chemistry Department, The Ohio State University, 120 West 18th Avenue, Columbus, Ohio 43210. *Received March 30, 1987*

Abstract: An entirely new family of lacunar Schiff base nickel(II) complexes is reported. The new species provide a protected void or lacuna in the vicinity of a coordination site at the metal ion, which may facilitate reversible O_2 binding by derivatives of appropriate metal ions. The lacunar ligands are prepared by adding a long bridging group that spans the plane of the well-known Schiff base ligand bis(acetylacetone)ethylenediamine. The bridging linkage, which serves as the roof of the lacuna, contains aromatic groups as risers linked to polymethylene chain through heteroatoms that provide flexible points within the bridge structure. Ease of synthesis has been a consideration in ligand design. Two crystal structures have been determined on nickel(II) derivatives of ligands of this class. The results show that the orientation of the roof of the lacuna relative to the approximately planar parent Schiff base ligand is dependent on the substituents on the β-diketone moiety. $[Ni(Me_2R^2Me_2malen)]\cdot 2CHCl_3$ crystallizes in the monoclinic space group $P2_1/c$ with $a = 10.608$ (2) Å, $b = 18.388$ (4) Å, $c = 20.492$ (4) Å, $\beta = 95.35$ (2)°, and $Z = 4$. The structure refined to $R = 0.051$ and $R_w = 0.050$ for 4078 reflections with $F_o^2 > 3\sigma(F_o^2)$. The bridge projects above the coordination plane giving a substantial cavity. Solvent molecules flank the cavity. $[Ni(Me_2R^2H_2malen)]\cdot CH_2Cl_2$ is in monoclinic space group $P2_1/n$ with $a = 13.205$ (3) Å, $b = 17.497$ (3) Å, $c = 14.315$ (5) Å, $\beta = 93.59$ (2)°, and $Z = 4$. $R = 0.106$ and $R_w = 0.092$ for 3496 reflections with $F_o^2 > 3\sigma(F_o^2)$. The bridge is not held vertically above the coordination plane. The difference in structures is attributed to the presence or absence of pairs of methyl groups on the β-diketone moieties.

The evolution of the broad chemistry of macrocyclic ligands constitutes one of the major pillars[1] of the enormous research subject bearing the title "inclusion chemistry".[2] Metal coordination by such entities constituted the principal activity during the founding years for that part of the field that derived from early

(1) See: Izatt, R. M., Christensen, J. J., Eds. *Advances in Macrocycle Chemistry*; Wiley: New York, 1987; Vol. 3, and reviews and references therein.

(2) Broadly defined, inclusion chemistry incorporates all those chemical species, whether they be continuous solids or discrete molecules, having voids or cavities of molecular dimension, and all of the related chemical association and other reaction chemistry. Implicit in the name is the capability of *including* some other molecular entities within the cavities.

0002-7863/88/1510-1480$01.50/0